Influence of substrate metal alloy type on the properties of hydroxyapatite coatings deposited using a novel ambient temperature deposition technique

J. N. Barry[1], A. Cowley[2], P. J. McNally[2] and D. P. Dowling[1]

[1] School of Mechanical & Materials Engineering, University College Dublin, Belfield, Dublin 4, Ireland

[2] School of Electronic Engineering, Dublin City University, Dublin 9, Ireland

Abstract

Hydroxyapatite (HA) coatings are widely applied to enhance the level of osteointegration onto orthopaedic implants. Atmospheric plasma spray (APS) is typically used for the deposition of these coatings, however HA crystalline changes regularly occur during this high thermal process. This paper reports on the evaluation of a novel low temperature (<47 °C) HA deposition technique, called CoBlast, for the application of crystalline HA coatings. To-date, reports on the CoBlast technique have been limited to titanium alloy substrates. This study addresses the suitability of the CoBlast technique for the deposition of HA coatings on a number of alternative metal alloys utilised in the fabrication of orthopaedic devices. In addition to titanium grade 5, both cobalt chromium and stainless steel 316 were investigated. In this study HA coatings were deposited using both the CoBlast and plasma sprayed techniques, and the resultant HA coating and substrate properties were evaluated and compared. The CoBlast deposited HA coatings were found to present similar surface morphologies, interfacial properties and composition irrespective of the substrate alloy type. Coating thickness however displayed some variation with the substrate alloy, ranging from 2.0 to 3.0 μm. This perhaps is associated with the electro-negativity of the metal alloys. The APS treated samples exhibited evidence of both coating, and significantly, substrate phase alterations for two metal alloys; titanium grade 5 and cobalt chrome. Conversely, the CoBlast processed samples exhibited no phase changes to the substrates after depositions. The APS alterations were attributed to the brief, but high intensity temperatures experienced during processing.

Keywords: Low temperature depositions process, Deposition of crystalline hydroxyapatite coatings, Metal alloy substrate evaluations, Thermally affected substrates, Residual alumina grit.

1 Introduction

Hydroxyapatite (HA) is a calcium phosphate apatite which has a chemical composition similar to the mineral phase of naturally occurring bone and is classified as osteo-conductive [1-5]. These attributes have led to the broad application of HA in both the orthopaedic and dentistry fields [3-6]. Despite its biological properties however, the bulk mechanical properties of HA are inadequate for load bearing applications [1,5]. In its bulk form HA is brittle, has poor tensile strength and low impact resistance [1,5]. Consequently HA is more often used as a coating to enhance the biological response of orthopaedic implants, while the durability and mechanical functionality is retained in the device's metallic substrate [1,2,7].

The metal alloys typically used in the fabrication of cement-less orthopaedic implants are; titanium grade 5, stainless steel 316 and cobalt chrome [1,8,9]. The HA coating of such implants are typically performed using a thermal spray technique called atmospheric plasma spray (APS) [5,6,10,11]. The ability to deposit HA onto a broad range of metal alloy substrates is an important feature of the APS technique, making this an important processing consideration for any alternative deposition technology. A concern with the APS technique for HA coating deposition however, is the high residual stresses within the coatings, as well as uncontrolled changes in HA crystallinity that can occurs during the high temperature deposition process (approx. 6000K) [1,5,11-16]. For example if a reduction in HA crystallinity occurs, it can result in coatings with higher dissolution rates (ie increase material lose) and thus reduced long term fixation *in vivo* [1,17,18]. Further to this, reports have suggested that this type of thermal deposition process can significantly affect the substrate properties [16,19-21]. As a consequence, there has been increased interest in alternative deposition techniques, which minimize the thermal impact on both the powder and substrate material [11].

This paper reports on a recently developed microblasting technique for the application of HA coatings onto metallic substrates called CoBlast [22]. The CoBlast technique utilises two particle jets

entrained in dry compressed air, one consisting of HA particles and the second, particles of a suitable abrasive media. These jets coincidently impinge on a point at the substrate surface resulting in the deposition of a HA coating. To date reports on the CoBlast HA deposition process have focused primarily on titanium and its alloys [23-29]. The aim of this research is to investigate the potential of the CoBlast HA deposition technique for use with a broader range of metal alloys, specifically: cobalt chrome and stainless steel 316. Furthermore, the substrate-HA interface of the CoBlast treated samples will be benchmarked against those obtained using the APS process for the same metal alloy substrates.

2 Materials and Method

2.1 Materials and Sample preparation

HA powder with particle size in the range 25-60 µm was purchased from S.A.I. (Science Applications Industries, France). To remove any retained moisture that may hinder powder flow, the HA powder was heated to 150°C for 1.5 hours prior to the deposition experiments. Al_2O_3 powder (with mean particle size of 100 µm) was purchased from Comco (USA) and was utilised as an abrasive in conjunction with the HA for the CoBlast process.

The deposition studies were performed on circular coupons of titanium grade 5 (Ti), stainless steel 316 (SS) and cobalt chrome (CoCr) alloys, with diameters of approx. 20 mm and thicknesses greater than 5 mm. Prior to coating, the test substrates were polished with 1200 grit silicon carbide paper, followed by ultrasonic cleaning consecutively with methanol and acetone for 5 minutes each.

The APS HA coatings were obtained from a commercial supplier of coatings to the medical device sector. The depositions were carried out with the same HA powder and substrates as used with the CoBlast process. These coatings were found to have an average thickness of approx. 55 µm, which

was independent of the substrate alloy. This was to be expected as the thickness of is dependent of the number of deposition passes executed [1].

2.2 Deposition equipment

The CoBlast deposition applicator (Figure 1) consists of the abrasive and HA jet applicator nozzles mounted in a sealed glove box, above an X-Y slide table. This facilitates motion of the substrates beneath the applicator, which coincidentally blasts the air jets, with entrained particles, at a point on the substrate surface. A containment bag encloses the working environment in which the deposition process is conducted. The HA and abrasive powders are delivered to an area on the titanium surface (or 'blast-zone') through the applicator nozzles using two Comco Accuflo powder feeders.

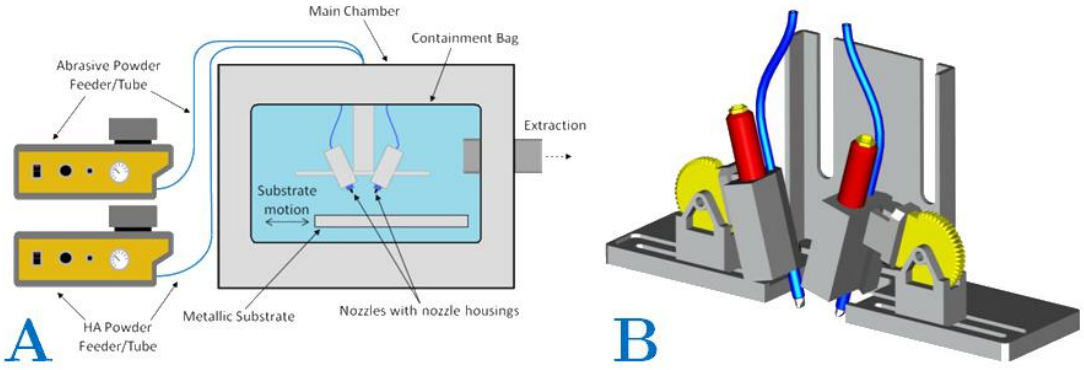

Figure 1: A) Schematic of the CoBlast deposition equipment, B) Schematic of the dual nozzle CoBlast applicator

Preliminary deposition studies focused on optimising HA coating coverage and homogeneity. The optimised deposition conditions using both the HA and Al_2O_3 powder are given in Table 1. The coatings were applied by passing the prepared substrates through the coincident blast-zone, using a 2 mm raster pattern at ≈10 mm/s. Following CoBlast processing, the samples were immersed in deionised water and ultrasonically cleaned for 5 minutes to remove any residual non-adhered HA particles. The samples were then dried in an oven at 50 °C.

Table 1: Deposition parameters for the CoBlast deposited HA coating

Powder	Mean Particle size (μm)	Nozzle Angle (°)	Height (mm)	Pressure (kPa)
HA	25-60	80	20	590
Al_2O_3	100	80	20	415

2.3 HA Coating and substrate analysis

A TM-1000 Hitachi scanning electron microscope (SEM), operating in back-scatter mode, was utilised to examine the coating morphologies and cross sections. Surface morphology and cross sectional images were taken at 8 random points on 3 samples of each coating. Digimizer software (MedCalc Software, Mariakerke, Belgium) was employed on the cross sectional images to facilitate HA coating thickness data to be obtained. The samples were prepared for cross sectional imaging by mounting in polyester resin blocks, cutting transverse sections and polishing the sections to a sub-micron finish.

A WYKO NT1100 optical profilometer, operating in vertical scanning interferometry (VSI) mode with a resolution of 3 nm per individual measurement, was utilised to measure the roughness component (R_a: Arithmetic average) of the HA coating. Measurements were taken at a magnification of x51.5, over 10 random areas (area dimensions: 120 x 91μm) on 4 samples of each HA coating type. To further facilitate the examination of the substrate under the CoBlast and APS HA coatings, the HA layers were removed by immersion in a 1M HCl solution for up to 3 minutes. Roughness measurements were obtained of the metal substrates after washing in deionised water followed by drying.

2.4 Chemical and crystallinity analysis

Elemental analysis was carried out using an EDX (Swift-ED, Oxford Instruments Analytical) module attached to the Hitachi SEM, operating at an acceleration voltage of 15kV and a magnification of x200. EDX was obtained for 8 random points on 3 samples of each coating, using a raster scan to obtain an average of elements present.

X-Ray Diffraction (XRD, Siemens D500 system) was performed to assess coating crystallinity. HA coatings deposited using both the CoBlast and APS technologies were analysed over the detector range of 25° to 35° with a resolution of 0.02° and a grab time of 3 seconds. The XRD scans were also carried out on compressed tablets of the HA precursor powder for comparison to the obtained HA coating spectra. In addition, XRD was performed over the detector range of 25° to 60° on the CoBlast and APS treated substrates after HCl etching (1 M), to examine each of the substrate metal alloys crystallography before and after the deposition treatements. MAUD (Materials Analysis Using Diffraction), a spectra fitting software, was utilised to evaluate the XRD spectra obtained for both the HA coatings and substrates [30-33].

2.5 Mechanical Testing

Micro-hardness values for the three metal alloy substrates were obtained using a leitz Knoop indentor. A 5 N load was applied, via the Knoop diamond tip, into the substrate. A total of 5 indentations were performed per substrate, at a standard indentation period of 5 seconds. The width of the indentations was evaluated using an Olympus GX51 digital optical inverted microscope, and facilitated the determination of micro-hardness values for each of the substrates.

The adhesion of the CoBlast deposited coatings were assessed using a scratch testing technique, which involved pre-loading a Vickers diamond tip to 5 N on the coated surface, and gradually increasing the load (100 N/min) up to 120 N, while the tip traverses across the coating at 10 mm/min. This type of adhesion testing is performed typically on thin, smooth and uniform coatings such as those deposited using PVD, however, the scratch test is considered adequate for a comparative assessment of adhesion performance on coatings provided the comparison is between coatings deposited using the same technology [34]. The failure criterion for this test, occurred when complete removal of the HA material from the substrate surface was achieved. The total length of the scratch is term Total Scratch Length (SL_T) and the length to failure of the coating is termed Coating Scratch

Length (SL_C). It is the ratio of these components, SL_C/SL_T, multiplied by the change in force (ΔF, Max force – Pre-loaded force) which determines the Critical Failure Load (L_{CF}).

$$L_{CF} = (SL_C/SL_T) \times \Delta F$$

3 Results and Discussion

In this section the properties of the CoBlast HA coatings deposited on titanium grade 5, stainless steel 316 and cobalt chrome are firstly compared. Subsequently the focus is on benchmarking the CoBlast coatings with APS deposited HA coatings applied onto the same alloy substrates. The study included an investigation of coating morphology, their adhesion to the substrate surface, cross-sectional examination and phase/compositional analysis. An assessment of the substrate micro-hardness is also carried out.

3.1 Morphology and Substrate Microhardness

Figure 2A and B display typical coating morphologies (SEM) and line profiles (optical profilometry) for the CoBlast deposited HA coatings on the three metal substrates. The SEM micrographs indicate that the CoBlast deposited HA coatings exhibit similar morphologies irrespective of the substrate material. The line profiles (Figure 2B) however, suggest some variation exists between the coated substrates, with deeper indentations observed on the SS coated substrates, when compared to the CoCr and Ti coated substrates. These indentations are linked to the abrasive action inherent in the CoBlast process, due to impact and removal of material by the Al_2O_3 powder grains. To better understand these results, a comparative optical profilometry study was performed on both the coated and metal substrate after coating removal.

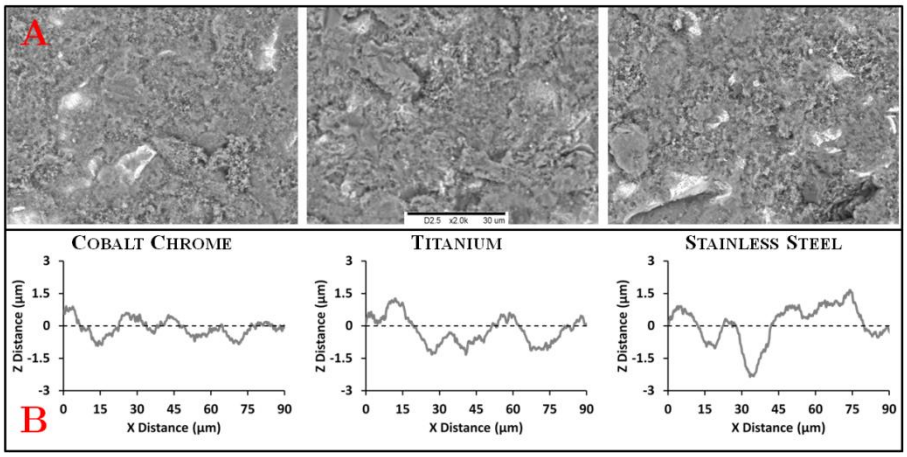

Figure 2: SEM images (A) and line profile scans (B) of the CoBlast HA coatings on the three metal substrates evaluated (Scale bar = 30 µm)

Figure 3 and Figure 4 provide details on the roughness (R_a and R_t respectively) obtained for the CoBlast deposited HA coatings on the three substrate types. The R_a values were found to increase in the following substrate order: cobalt chrome < titanium < stainless steel. The HA coatings were removed by dissolution in 1M HCl. Figure 3 also provide details on the roughness data obtained for the substrates. The R_a values for the latter were slightly reduced when compared to their respective coated samples, but still followed a similar trend to that of the coated samples. Furthermore the roughness results validate the suggestion that the SS substrates were most affected by the abrasive action, as this substrate exhibited the highest roughness for both the coating and substrate. In order to investigate these micro-hardness measurements were carried out on each substrate to determine if substrate hardness had an influence on the roughness obtained after the CoBlast treatment.

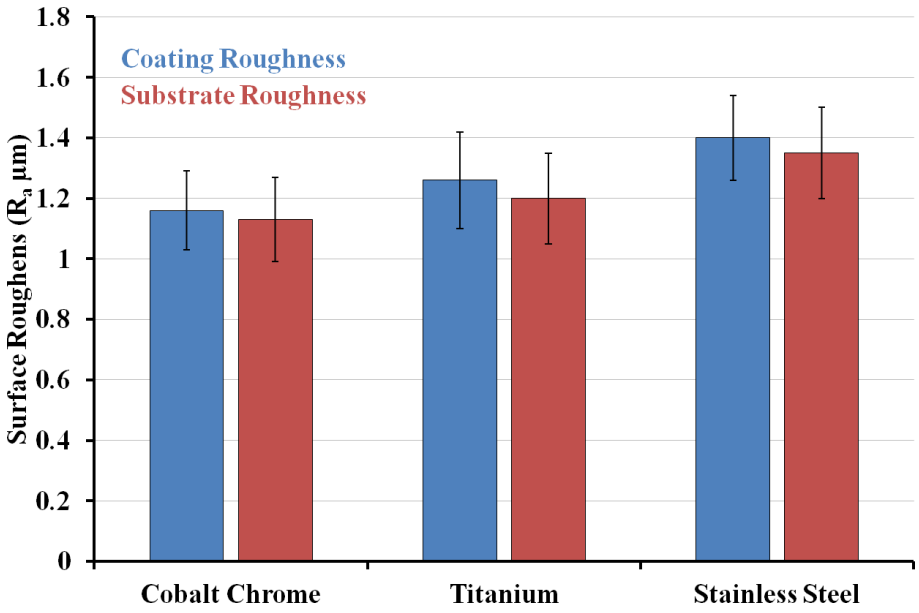

Figure 3: Roughness (R_a) results for CoBlast deposited HA on the metallic substrates shown, also shown is the roughness of the substrate beneath after HA removal

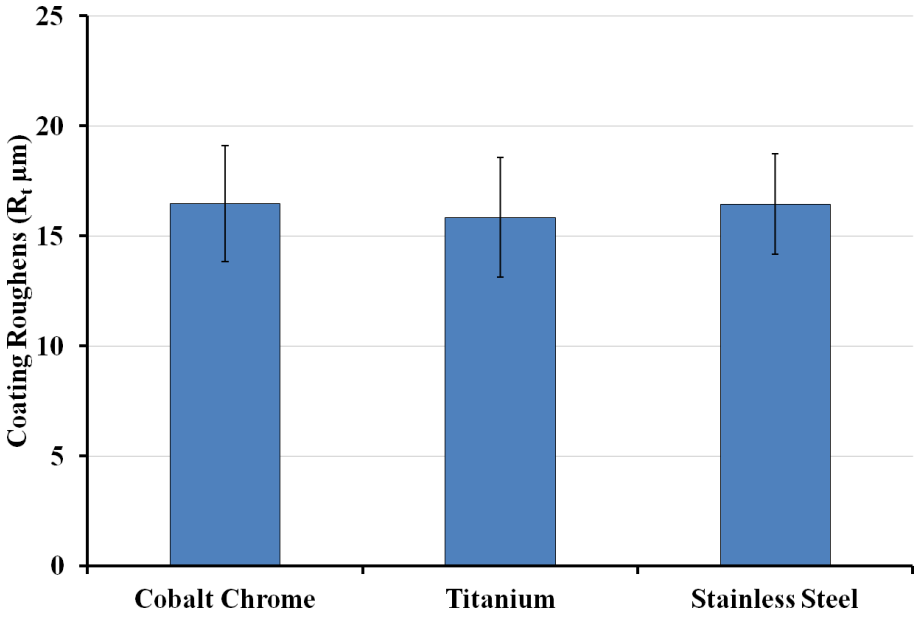

Figure 4 Roughness (R_t) results for CoBlast deposited HA on the metallic substrates

The substrate microhardnesses results in Figure 5 were determined using the knoop indentation technique. The microhardness results demonstrated a close correlation with the substrate roughness, where a decrease in roughness was mirrored by an increase in microhardness. It is possible this relationship stems from the abrasive 'chipping action' functioning at the micron level, due to the

abrasive particle's size, where the microhardness might best represent the mechanical properties of the substrate at this level. This would explain why the material with the lowest microhardness, stainless steel, exhibited the roughest surface finish after the CoBlast treatment.

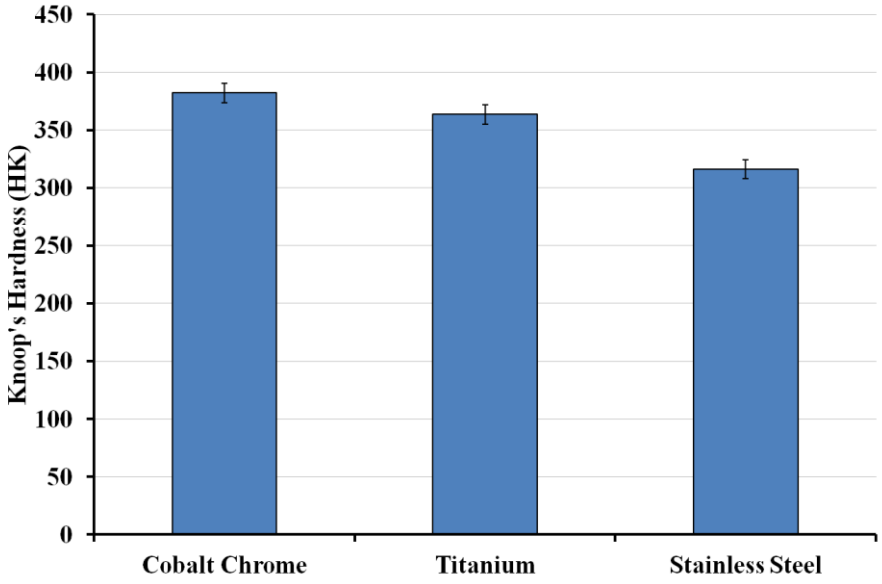

Figure 5: Knoop micro-hardness values for the three metal alloy substrates

3.2 Coating Thickness

The thickness of the CoBlast deposited HA coatings on each of the metal alloy substrates were obtained based on cross sectionals examination (Figure 6), combined with the use of Digimizer software. Considerable variation in coating thickness was observed due to the roughness of the blasted metal alloys, the thickness values obtained are based on an average of 64 measurements on each coating. The HA coatings deposited onto the titanium substrates were found to have an average coating thickness of 3.0 µm, compared to the 2.0 and 2.3 µm coatings deposited on the cobalt chrome and stainless steel substrates (Figure 7). It is important to note, that while the CoBlast deposited HA coating thickness varies across the metal substrate surface, based on optical microscopy examination, there was no evidence of uncoated areas.

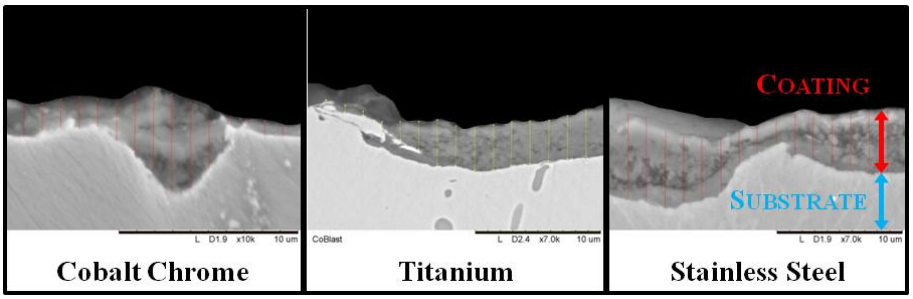

Figure 6: Typical SEM cross sectional micrographs of the HA coatings on the three substrates (Scale Bar = 10µm)

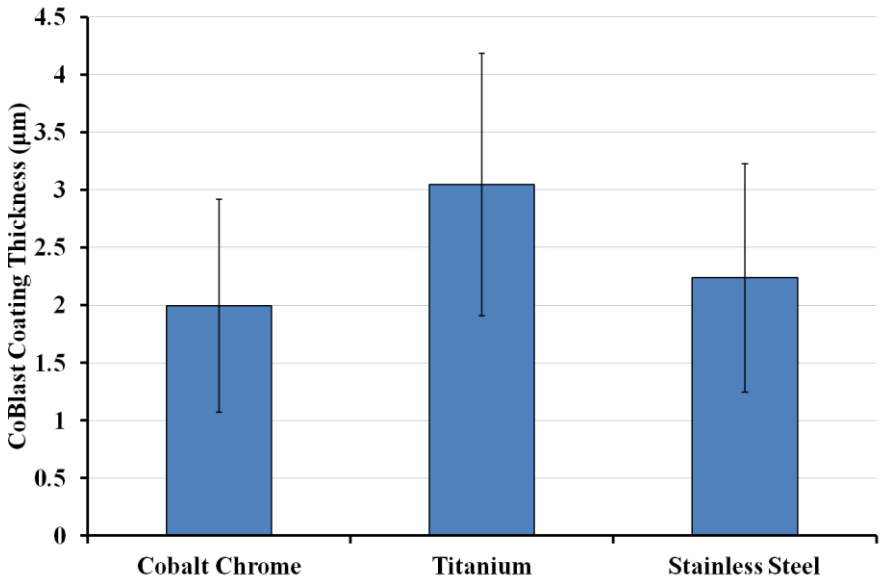

Figure 7: Variation in HA coating thickness obtained on the three substrate surfaces determined using the Digimizer software

The increased HA thickness observed on the Ti substrates may be associated with its enhanced reactivity to oxidation, due to the greater variance in 'Pauling Electronegativity' between titanium and both oxygen and hydrogen [35]. This enhanced reactivity may in turn facilitate a higher level of bonding to the oxygen and hydroxyl functional groups within the HA molecules [35]. It has been reported previously that the adhesion of the CoBlast deposited HA coating may be a combination of mechanical interlocking and 'mechano-chemical bonding', which is a type of chemical bonding brought about by specific mechanical interactions [36,37]. This type of functional bonding would

support the suggestion that Pauling Electronegativity is a contributing factor in the bonding process [25,35-38].

3.3 Coating adhesion

As detailed in Figure 8 the scratch test results for the CoBlast deposited HA coatings, show broadly similar coating failure loads independent of the substrate metal alloy, with average values ranging from 52 to 63 N. In contrast to the coating delamination failure mechanism often observed for PVD coatings, no significant delamination was observed to the coating around the scratch. The failure points of the coatings were confirmed using EDX, which showed a significant drop in the presence of Ca and P (constituent elements in HA), at the base of the scratch's. The results suggest the adhesion of the CoBlast deposited HA coating is independent of the substrate metal alloy. The marginally higher level in the mean coating failure load for the HA coatings deposited on the titanium alloy substrate may be associated with the titanium's enhanced reactivity to oxidation, as discussed previously [25,35,38].

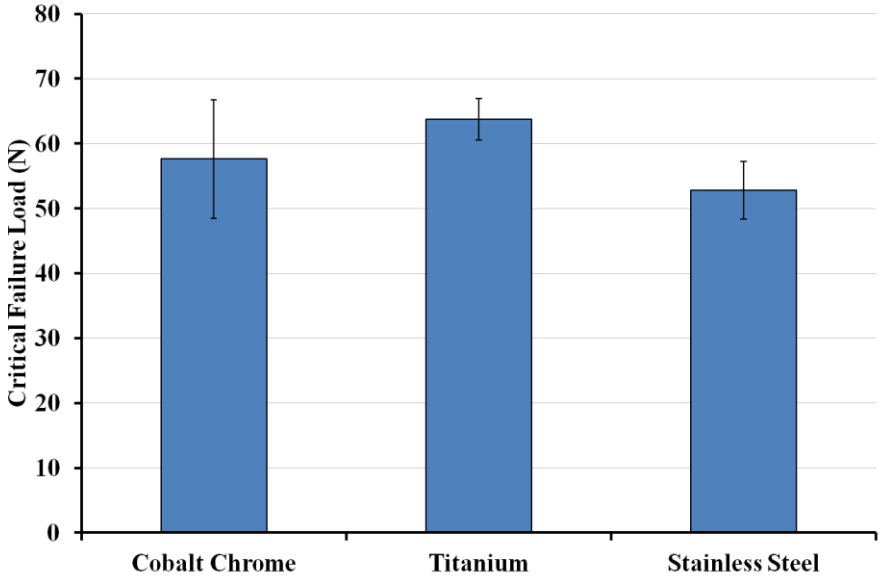

Figure 8: Scratch adhesion test results for the CoBlast HA coatings on each of the substrate types as shown

3.4 APS Coatings

Having provided details on the APS coating morphology, thickness and adhesion on the CoBlast deposited HA coatings, this section provides information on the APS deposited HA coatings on the same substrates [29]. Evaluation of the APS HA coating thickness (Figure 9) found that each of their thickness values fell within the optimum thickness range of between 50 and 70 μm, which is reported to help avoid fatigue failure and embrittlement of the coating [16,39-41]. It was also apparent from Figure 9 that each of the APS deposited coatings have similar thickness values irrespective of the substrate materials utilised in their deposition. Indicating the coating property, coating thickness, is independent of the substrate material. This independence of the substrate material is attributed the APS technology's high process temperature (approx. 6000 K), allowing most ceramic materials to be heated to a molten form and deposited onto most substrate surface capable of withstanding the process's thermal properties. This reflects the difference between the CoBlast and APS technologies, where the former's coating properties are influenced by the substrate material properties as detailed in this paper amongst. As previously highlighted however, there are concerns regarding the affect this high processing temperature has on the properties of the APS deposited HA coating [1,5,11-16]. The composition of both the HA coatings and the substrate beneath were assessed using EDX and XRD, and a comparison was drawn between the CoBlast and APS treated samples.

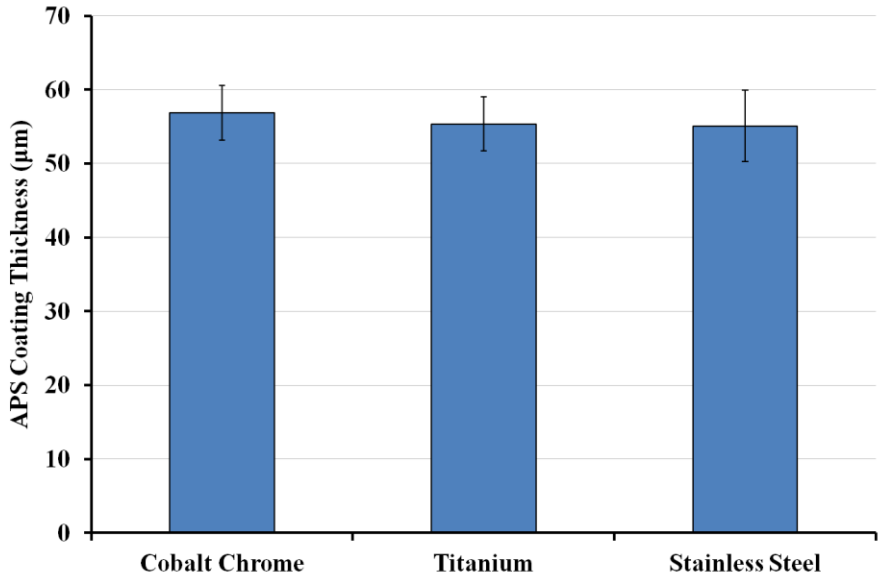

Figure 9: APS HA coating thickness obtained on the three substrate surfaces determined using the Digimizer software

3.5 Compositional Analysis of the CoBlast and APS Deposited Coatings

Energy-dispersive X-ray spectroscopy (EDX) analysis was performed on each of the CoBlast deposited HA coatings to determine if the deposition process affected the composition of the HA materials. The results of the EDX elemental analysis are shown in Table 2. These results show that for each of the CoBlast deposition HA coatings, the EDX technique detected elements present in the substrate through the coating. This is due to the EDX X-ray penetration depth of up to 4 µm (system operated at 15 kV fixed acceleration voltage), which is greater than the thickness of the CoBlast deposited HA coatings (see Figure 7) [25]. Based on the EDX analysis, an average weight percent ratio of 2.2 for calcium to phosphorous (Ca/P) was obtained for the CoBlast coatings, this is close to the ratio of 2.1 for the precursor HA powder. In contrast, EDX evaluation of the APS coatings found an average Ca/P ratio of 2.9 for the HA coatings on all three substrates, suggesting similar levels of chemical alterations had occurred on each of the substrates during the APS deposition process.

Table 2: EDX results obtained for the CoBlast and APS HA coatings deposited on each of the metal alloy substrates

Material	Calcium (Wt%)	Phosphorous (Wt%)	Substrate (Wt%)
CoBlast (CoCr)	47.7	22.6	29.7
CoBlast (Ti)	48.8	21.1	30.3
CoBlast (SS)	49.1	22.0	28.9
APS (All substrates)	74.3	25.8	-
Powder	67.3	32.7	-

An X-Ray Diffraction (XRD) study was carried out on each of the HA coatings and treated substrates alloys after etching of the HA coating. As demonstrated by the XRD spectra given in Figure 10, the CoBlast deposited HA coatings on the three substrate alloys exhibit a crystalline structure similar to that of the precursor HA powder (as is supported by the EDX results). Their peak positions and intensities match those of the precursor HA powder spectrum. This was quantified and verified using MAUD analysis software [30-33], demonstrating that the low temperature deposition process of the CoBlast technique allows the crystallinity of the precursor HA powder to be retained regardless of the substrate alloy. Prevéy reported the XRD peak broadening, displayed in each of the HA coating spectra, may be due to the existence of nanocrystalline HA [42].

XRD of the APS HA coatings were compared with those obtained using the CoBlast process. While the APS coating exhibit's similar peaks to the precursor HA powder, the MAUD analysis software estimates greater than 9 wt. % of the HA coating has been converted to alternative calcium phosphate phases, such as; tri-calcium phosphate (TCP), tetra-calcium phosphate (TTCP). The presence of the 'amorphous halo' (highlighted in Figure 10), associated with amorphous HA, indicates further deviation from the precursor HA powder has occurred during processing [1,43-46]. The amorphous content in the coating was however not quantifiable using the MAUD software due to inherent limitation in the software [30-33,44]. It should be noted that calcium phosphate phases such as; TCP, TTCP and amorphous HA, are known for their increased dissolution rates, which has been reported

to allow for rapid osseointegration, when compared with the pure HA. These phases however, are generally associated with rapid bone formations [1], rather than stable, lamellar bone observed previously for CoBlast coatings [25]. Significantly, the XRD spectra for the APS processed titanium and stainless steel substrates mirrored that of the cobalt chrome spectrum shown in Figure 10, verifying that thermal modification of the HA powder occurs irrespective of the substrate alloy type [1].

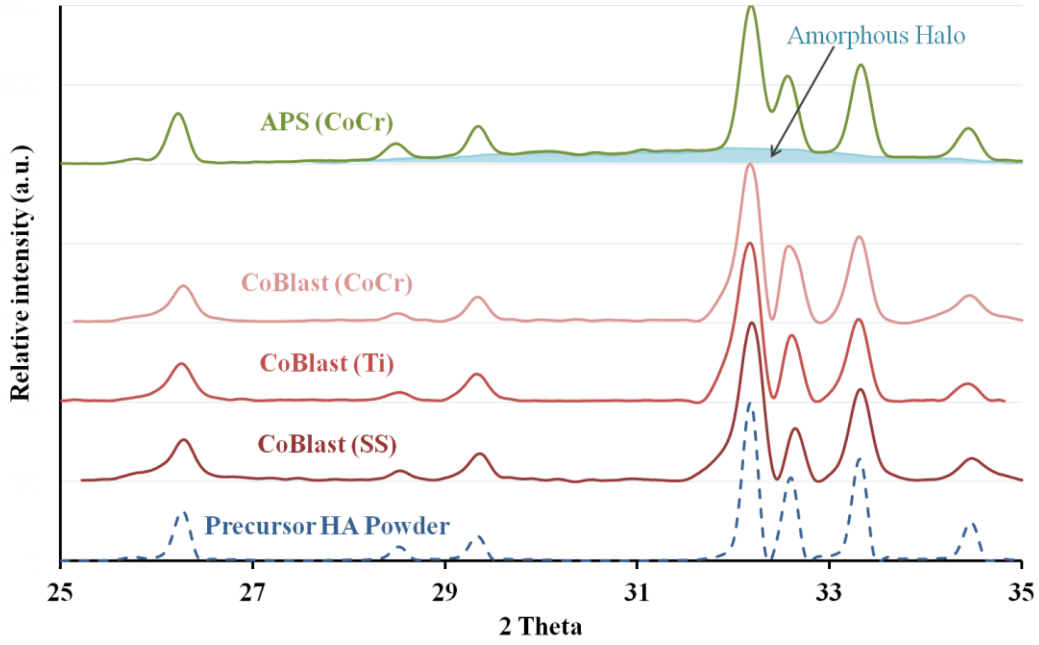

Figure 10: The XRD spectra of the HA powder and CoBlast deposited HA coatings on the three substrate alloys

The substrate spectra in Figure 11 relate to the XRD evaluation of the alloy substrates onto which the deposited HA coatings have been applied. The evaluation of the substrates was facilitated by removal of the HA coating via acid etching as detailed earlier. From Figure 11, it is clear that the CoBlast processed substrates experience no significant change in crystal structure, as their peak positions and intensities match those of the 'Bare' unprocessed substrates. This was verified by MAUD analysis, where the 'Bare' and CoBlast processed substrates were found to have similar weight percentages of substrate associated phases present. This again demonstrates the minimally invasive nature of the low temperature CoBlast deposition process with respect to the metal substrate phase composition. In

contrast, MAUD analysis of the APS processed substrates established that phase alterations were exhibited in both the titanium and the chrome substrates. In the case of the latter, for example, peaks located at 47.1° and 51° were no longer identified in the metal alloy substrate spectra after the APS HA processing. The changes which occur in the titanium and cobalt chrome have been shown previously to be associated with high deposition temperatures, and have been suggested to significantly alter the mechanical performance of the metal alloys [47]. Stainless steel however, was unaffected by APS processing. This was attributed to the high transus temperature (temperature where phase transition initiates) of the stainless steel alloy (<1050 °C) relative to titanium (<880 °C) and cobalt chrome (<890 °C) alloys [48]. Below this transus temperate, the stainless steel alloy would maintain its phase composition including, its FCC structure, while phase changes would have initiated in the titanium and cobalt chrome alloy substrates almost 200 °C below the temperature at which this occurs for the stainless steel substrates [48].

Significantly, there are 5 distinct peaks which occur in the APS processed samples (asterisks * in Figure 11), which are not present in either the uncoated or CoBlast processed substrates (with the exception of one overlapping peak in the titanium alloy spectrum). It was determined these peak represent the presence of Al_2O_3 contaminant, typically utilised in the pre-processing stages of the APS process [49]. This was verified by MAUD analysis, indicating that Al_2O_3 could account for as much as 22 wt% of phases present at the HA/substrate interface, cross sectional SEM and spot EDX was also employed to confirm the presence of this material. Figure 12 shows a cross sectional micrograph, where an embedded Al_2O_3 particles is evident and the result of the spot EDX evaluation is given. This was also observed by Garcia-Sanz et. al. [50]. It is interesting to note that despite Al_2O_3 powder being used as an abrasive for the CoBlast process, no significant levels of Al_2O_3 was detected in the deposited HA coatings, as highlighted previously [25,38,51]. The XRD findings are in agreement with previous work carried out on titanium grade 5 substrates with APS deposited HA coatings, where similar levels of both HA and substrate phase alterations were observed.

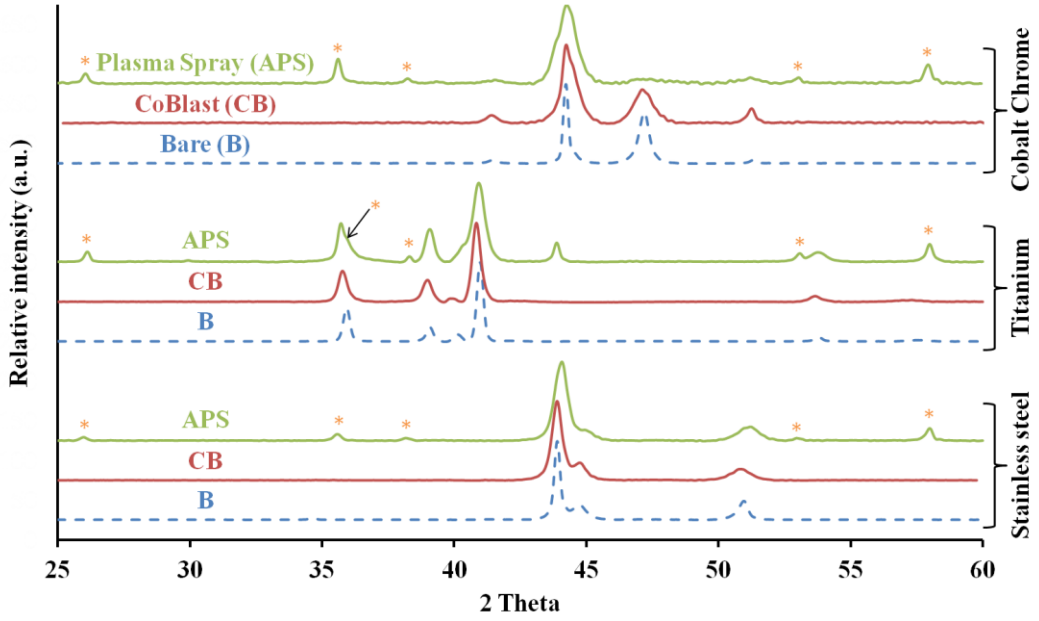

Figure 11: XRD spectra for the three substrates after HA removal. The peaks indicated by * were neither observed in the bare substrate or the HA coatings

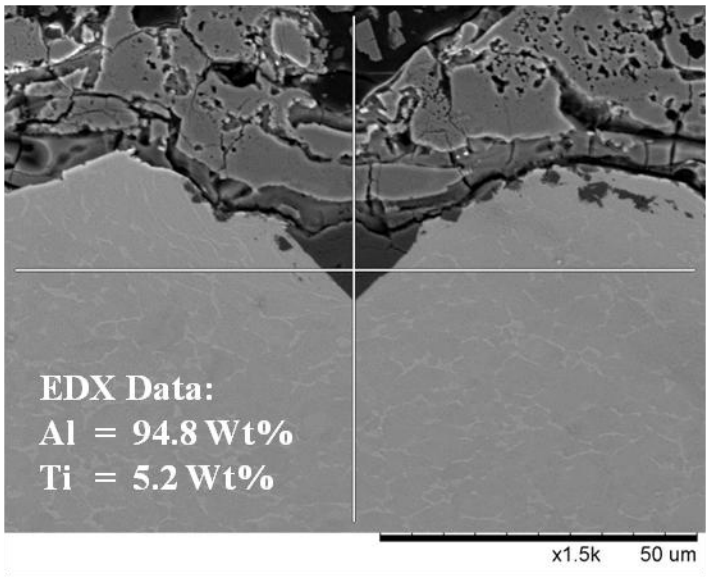

Figure 12: SEM cross section of an APS deposited HA coating exhibiting an Al_2O_3 particle embedded in the titanium alloy substrate beneath the coating, Spot EDX data of the cross-hairs location is given also

4 Conclusions

In this study the influence of substrate alloy type (cobalt chrome, titanium grade 5 and stainless steel) was investigated with respect to its effect on the properties of HA coatings deposited using the CoBlast technique. The HA coated alloys were found to present similar interfacial properties and coating composition irrespective of alloy type, however, surface roughness and coating thickness were observed to vary between the three substrate types. The trend of increased roughness of cobalt chrome > titanium > stainless steel, appears to correlate with the micro-hardness of the alloys, with higher micro-hardness it is likely that the alloy will exhibit higher resistance to particle abrasion on the micro-scale. The variation in coating thickness may be associated with the Electronegativity of the different metal alloys examined, were a greater difference in Pauling Electronegativity to oxygen could explain the higher level of reactivity with the HA. The crystallinity of the CoBlast deposited coatings were observed to matched those of the precursor HA powder, demonstrating that the CoBlast deposition process did not affect the crystal structure of the HA, in addition, it was also observed not to affect the substrate's crystal structure. Conversely, the XRD analysis showed that the titanium and cobalt chromium substrates were altered by the high temperature APS technique, and furthermore the deposited HA was modified when compared to that of the precursor HA powder. The advantage of the CoBlast process therefore is the minimal alteration observed for both the HA coating and substrate alloys, with a further advantage being the absence of significant levels of Al_2O_3 in the CoBlast processed substrates. In contrast Al_2O_3 is presented in the APS deposited coating due to the abrasive pre-treatment used, which if not managed correctly could lead to third body wear of a device during implantation. In conclusion, this investigation demonstrates the suitability of the CoBlast technique in successfully deposit HA coating onto stainless steel and cobalt chrome alloys used routinely in the orthopaedic industry, in addition to the titanium grade 5 substrates previously investigated.

Acknowledgement: This research was supported by Science Foundation Ireland under Grant No.08/SRC/I1411

References

1. Hench LL, Wilson J. An introduction to bioceramics: World Scientific Pub Co Inc; 1993.
2. Paital SR, Dahotre NB. Calcium phosphate coatings for bio-implant applications: Materials, performance factors, and methodologies. Materials Science & Engineering R-Reports 2009;66(1-3):1-70.
3. Wang H, Eliaz N, Xiang Z, Hsu HP, Spector M, Hobbs LW. Early bone apposition in vivo on plasma-sprayed and electrochemically deposited hydroxyapatite coatings on titanium alloy. Biomaterials 2006;27(23):4192-203.
4. Sun L, Berndt C, Gross K, Kucuk A. Material fundamentals and clinical performance of plasma sprayed hydroxyapatite coatings: A review. Journal of biomedical materials research 2001;58(5):570-592.
5. Groot K, Wolke J, Jansen J. Calcium phosphate coatings for medical implants. Proceedings of the Institution of Mechanical Engineers, Part H: Journal of Engineering in Medicine 1998;212(2):137-147.
6. Lucas L, Lacefield W, Ong J, Whitehead R. Calcium phosphate coatings for medical and dental implants. Colloids and Surfaces A: Physicochemical and Engineering Aspects 1993;77(2):141-147.
7. Gu YW, Khor KA, Cheang P. In vitro studies of plasma-sprayed hydroxyapatite/Ti-6Al-4V composite coatings in simulated body fluid (SBF). Biomaterials 2003;24(9):1603-11.
8. Long PH. Medical devices in orthopedic applications. Toxicologic pathology 2008;36(1):85-91.
9. Brunette DM. Titanium in medicine: material science, surface science, engineering, biological responses, and medical applications: Springer Verlag; 2001.
10. Ding SJ, Su YM, Ju CP, Lin JH. Structure and immersion behavior of plasma-sprayed apatite-matrix coatings. Biomaterials 2001;22(8):833-45.
11. León B, Jansen JA. Thin calcium phosphate coatings for medical implants: Springer Verlag; 2008.
12. McGrann RTR, Greving DJ, Shadley JR, Rybicki EF, Kruecke TL, Bodger BE. The effect of coating residual stress on the fatigue life of thermal spray-coated steel and aluminum. Surface & Coatings Technology 1998;108(1-3):59-64.
13. Tsui YC, Doyle C, Clyne TW. Plasma sprayed hydroxyapatite coatings on titanium substrates. Part 1: Mechanical properties and residual stress levels. Biomaterials 1998;19(22):2015-29.
14. Klein CP, Patka P, Wolke JG, de Blieck-Hogervorst JM, de Groot K. Long-term in vivo study of plasma-sprayed coatings on titanium alloys of tetracalcium phosphate, hydroxyapatite and alpha-tricalcium phosphate. Biomaterials 1994;15(2):146-50.
15. Inadome T, Hayashi K, Nakashima Y, Tsumura H, Sugioka Y. Comparison of bone-implant interface shear strength of hydroxyapatite-coated and alumina-coated metal implants. J Biomed Mater Res 1995;29(1):19-24.
16. Lynn AK, DuQuesnay DL. Hydroxyapatite-coated Ti-6Al-4V part 1: the effect of coating thickness on mechanical fatigue behaviour. Biomaterials 2002;23(9):1937-46.

17. Xue WC, Tao SY, Liu XY, Zheng XB, Ding CX. In vivo evaluation of plasma sprayed hydroxyapatite coatings having different crystallinity. Biomaterials 2004;25(3):415-421.
18. Sun LM, Berndt CC, Grey CP. Phase, structural and microstructural investigations of plasma sprayed hydroxyapatite coatings. Materials Science and Engineering a-Structural Materials Properties Microstructure and Processing 2003;360(1-2):70-84.
19. Forrest DJ, Shelton JC, Gregson PJ. Fatigue failure in a plasma sprayed hydroxyapatite coated titanium alloy. 1996; Toronto. p 324.
20. Evans SL, Gregson PJ. The Effect of a Plasma-Sprayed Hydroxyapatite Coating on the Fatigue Properties of Ti-6al-4v. Materials Letters 1993;16(5):270-274.
21. Clemens JA, Wolke JG, Klein CP, de Groot K. Fatigue behavior of calcium phosphate coatings with different stability under dry and wet conditions. J Biomed Mater Res 1999;48(5):741-8.
22. O'Donoghue JGSADCW, Haverty DLCCL; US-A- 4 950 505; WO-A-03/080140; WO-A-96/16611; WO-A1-02/102431, assignee. METHOD OF DOPING SURFACES. EP patent EP 2061629 B1. 2011.
23. O'Neill L, O'Sullivan C, O'Hare P, Sexton L, Keady F, O'Donoghue J. Deposition of substituted apatites onto titanium surfaces using a novel blasting process. Surface and Coatings Technology 2009;204(4):484-488.
24. Tan F, Nasiri M, Al-Rubeai M. In vitro osteoblastic cell activity on Bioglass-derived bioceramic surfaces deposited by a novel coblast technique. Journal of Biotechnology 2010;150(Supplement 1):S105-S105.
25. O'Hare P, Meenan BJ, Burke GA, Byrne G, Dowling D, Hunt JA. Biological responses to hydroxyapatite surfaces deposited via a co-incident microblasting technique. Biomaterials 2010;31(3):515-22.
26. Tan F, Naciri M, Al-Rubeai M. Osteoconductivity and growth factor production by MG63 osteoblastic cells on bioglass-coated orthopedic implants. Biotechnol Bioeng 2011;108(2):454-64.
27. Tan F, Naciri M, Dowling D, Al-Rubeai M. In vitro and in vivo bioactivity of CoBlast hydroxyapatite coating and the effect of impaction on its osteoconductivity. Biotechnol Adv 2012;30(1):352-62.
28. O'Sullivan C, O'Hare P, O'Leary ND, Crean AM, Ryan K, Dobson AD, O'Neill L. Deposition of substituted apatites with anticolonizing properties onto titanium surfaces using a novel blasting process. J Biomed Mater Res B Appl Biomater 2010;95(1):141-9.
29. Barry JN, Dowling DP. Comparison between the SBF Response of Hydroxyapatite Coatings Deposited Using both a Plasma-Spray and a Novel Co-Incident Micro-Blasting Technique. Key Engineering Materials 2012;493:483-488.
30. Lutterotti L, Matthies S, Wenk HR, Schultz AS, Richardson JW. Combined texture and structure analysis of deformed limestone from time-of-flight neutron diffraction spectra. Journal of Applied Physics 1997;81(2):594-600.
31. Lutterotti L, Chateigner D, Ferrari S, Ricote J. Texture, residual stress and structural analysis of thin films using a combined X-ray analysis. Thin Solid Films 2004;450(1):34-41.
32. Lutterotti L, Bortolotti M, Ischia G, Lonardelli I, Wenk HR. Rietveld texture analysis from diffraction images. Zeitschrift Fur Kristallographie 2007;26:125-130.

33. Lutterotti L. Total pattern fitting for the combined size-strain-stress-texture determination in thin film diffraction. Nuclear Instruments & Methods in Physics Research Section B-Beam Interactions with Materials and Atoms 2010;268(3-4):334-340.
34. Steinmann PA, Tardy Y, Hintermann HE. Adhesion Testing by the Scratch Test Method - the Influence of Intrinsic and Extrinsic Parameters on the Critical Load. Thin Solid Films 1987;154(1-2):333-349.
35. Pauling L. The Nature of the Chemical Bond, 3rd. New York 1960.
36. Beyer MK, Clausen-Schaumann H. Mechanochemistry: the mechanical activation of covalent bonds. Chem Rev 2005;105(8):2921-48.
37. Konopka M, Turansky R, Reichert J, Fuchs H, Marx D, Stich I. Mechanochemistry and thermochemistry are different: stress-induced strengthening of chemical bonds. Phys Rev Lett 2008;100(11):115503.
38. O'Neill L, O'Sullivan C, O'Hare P, Sexton L, Keady F, O'Donoghue J. Deposition of substituted apatites onto titanium surfaces using a novel blasting process. Surface & Coatings Technology 2009;204(4):484-488.
39. de Groot K, Wolke JG, Jansen JA. Calcium phosphate coatings for medical implants. Proc Inst Mech Eng H 1998;212(2):137-47.
40. de Groot K, Geesink R, Klein C, Serekian P. Plasma sprayed coatings of hydroxylapatite. Journal of biomedical materials research 2004;21(12):1375-1381.
41. Geesink RGT, Degroot K, Klein CPAT. Chemical Implant Fixation Using Hydroxyl-Apatite Coatings - the Development of a Human Total Hip-Prosthesis for Chemical Fixation to Bone Using Hydroxyl-Apatite Coatings on Titanium Substrates. Clinical Orthopaedics and Related Research 1987(225):147-170.
42. Prevéy PS. X-ray diffraction characterization of crystallinity and phase composition in plasma-sprayed hydroxyapatite coatings. Journal of Thermal Spray Technology 2000;9(3):369-376.
43. Gross KA, Walsh W, Swarts E. Analysis of retrieved hydroxyapatite-coated hip prostheses. Journal of Thermal Spray Technology 2004;13(2):190-199.
44. Gross KA, Berndt CC, Herman H. Amorphous phase formation in plasma-sprayed hydroxyapatite coatings. J Biomed Mater Res 1998;39(3):407-14.
45. Gross KA, Berndt CC, Stephens P, Dinnebier R. Oxyapatite in hydroxyapatite coatings. Journal of materials science 1998;33(15):3985-3991.
46. Berndt C, Gross K. Characteristics of Hydroxylapatite Bio-Coatings. Thermal Spray: International Advances in Coatings Technology 1992:465-470.
47. Pederson R. Microstructure and phase transformation of Ti-6Al-4V: Lulea University of Technology; 2002. 13 p.
48. Pilliar RM. Metallic biomaterials. In: Narayan R, editor. Biomedical Materials. Springer-Verlag US: Springer US; 2009. p 41-81.
49. Wigren J. Technical note: Grit blasting as surface preparation before plasma spraying. Surface and Coatings Technology 1988;34(1):101-108.
50. Garcia-Sanz FJ, Mayor MB, Arias JL, Pou J, Leon B, Perez-Amor M. Hydroxyapatite coatings: a comparative study between plasma-spray and pulsed laser deposition techniques. Journal of Materials Science: Materials in Medicine 1997;8(12):861-865.
51. Byrne GD, O'Neill L, Twomey B, Dowling DP. Comparison between shot peening and abrasive blasting processes as deposition methods for hydroxyapatite coatings onto a titanium alloy. Surface and Coatings Technology 2012.